Article

Pantothenate and L-carnitine Supplementation Corrects Pathological Alterations in Cellular Models of KAT6A Syndrome

Manuel Munuera-Cabeza[1], Mónica Álvarez-Córdoba[1], Juan M. Suárez-Rivero[1], Suleva Povea-Cabello[1], Irene Villalón-García[1], Marta Talaverón-Rey[1], Alejandra Suárez-Carrillo[1], Diana Reche-López[1], Paula Cilleros-Holgado[1], Rocío Piñero-Perez[1] and José A. Sánchez-Alcázar[1]*.

[1] Centro Andaluz de Biología del Desarrollo (CABD-CSIC-Universidad Pablo de Olavide), and Centro de Investigación Biomédica en Red: Enfermedades Raras, Instituto de Salud Carlos III, Sevilla 41013, Spain.

* José A. Sánchez Alcázar. Centro Andaluz de Biología del Desarrollo (CABD). Consejo Superior de Investigaciones Científicas. Universidad Pablo de Olavide. Carretera de Utrera Km 1, Sevilla 41013, Spain. Phone: 34 954978071. FAX: 34 954349376. Email: jasanalc@upo.es; Web page: http://www.upo.es/CABD/; Orcid: 0000-0001-9705-1469

Abstract: Mutations in several genes involved in the epigenetic regulation of gene expression have been considered risk genes to different intellectual disability (ID) syndromes associated with autism spectrum disorder (ASD) features including alterations of the lysine-acetyltransferase 6A (*KAT6A*) gene in KAT6A syndrome. KAT6A enzyme participates in a wide range of critical cellular functions such as chromatin remodeling, gene expression, protein synthesis, cell metabolism, and replication. In this manuscript, we examined the pathophysiological alterations in fibroblasts derived from three patients harboring KAT6A mutations. We addressed survival in stress medium, histone acetylation, protein expression patterns and transcriptome analysis as well as cell bioenergetics. In addition, we evaluated the therapeutic effectiveness of epigenetic modulators and mitochondrial boosting agents such as pantothenate and L-carnitine in correcting the mutant phenotype.

Pantothenate and L-carnitine treatment increased histone acetylation and corrected protein and transcriptomic expression patterns in mutant KAT6A cells. Furthermore, cell bioenergetics of mutant cells was significantly improved.

Our results suggest that pantothenate and L-carnitine can significantly correct the mutant phenotype in cellular models of KAT6A syndrome.

Keywords: intellectual disability; KAT6A syndrome; Lysine acetyltransferase 6 A; pantothenate; L-carnitine; histone acetylation

1. Introduction

Currently, the development of next-generation sequencing (NGS) techniques, numerous mutations in several genes involved in epigenetic regulation of gene expression have been considered risk genes to different intellectual disability (ID) syndromes often associated with autism spectrum disorders (ASDs) [1-5]. Among them, it has been included de novo mutations of the lysine-acetyltransferase 6A gene (*KAT6A*; a.k.a. *MYST3* and *MOZ*; MIM *601408) causing KAT6A syndrome (Arboleda-Tham Syndrome, autosomal dominant mental retardation 32; MIM # 616268) [6]. Autism and autistic features have been reported in approximately 25% of newly reported cases of KAT6A syndrome [1].

The *KAT6A* gene, located in chromosome 8p11.21, encodes a lysine-acetyltransferase 6A (KAT6A). KAT6A belongs to the MYST (named for members MOZ, Ybf2/Sas3, Sas2, and Tip60) family of histone acetyltransferases that are defined by the presence of a highly conserved MYST sequence consisting of a domain of binding to acetyl-CoA and a zinc finger motif [7]. The MYST family of proteins (KAT6A, KAT6B, KAT5 and KAT7)

 doi:10.20944/preprints202211.0273.v1

participate in many essential cellular processes, such as chromatin remodeling, regulation of gene expression, protein synthesis, metabolic pathways and cell division [8]. KAT6A function in a multisubunit complex with three other proteins: Bromodomain and PHD finger 1/2/3 (BRPF1/2/3), Inhibitor of growth family member 5 (ING5) and human Esa1-associated factor 6 (hEAF6) [9]. These proteins make a complex to acetylate lysine residues on histone H3 tails, that way regulating gene expression patterns and promoting diverse developmental programs.

KAT6A gene was identified at a frequent break-point of chromosomal rearrangements (translocations) associated with acute myeloid leukaemia (AML) [10]. KAT6A acetylates lysine-9 residues in histone H3 (H3K9), playing an essential role in transcriptional activity modulation and gene expression. KAT6A is also involved in the acetylation and regulation of the tumor suppressor p53, a multifactorial factor able to control cell cycle progression, DNA integrity and survival of the cells exposed to DNA damaging agents [11]. Moreover, KAT6A has the ability to bind and regulate several transcription factors such as Runx1 and Runx2 through its C-terminal domain [12].

Most of the reported mutations in KAT6A syndrome are autosomal dominant loss of function variants including splicing mutations, nonsense mutation, and frameshift changes. Recently, missense variants affecting critical conserved residues in functional domains have also been identified [1,13].

Most of the clinical features in KAT6A syndrome have a variable penetration (range of signs and symptoms that can occur in different people with the same genetic condition). The basic pathological characteristics are microcephaly, ID, autism, speech delay, cardiac alterations and gastrointestinal complications [1].

There are diverse experimental models to investigate KAT6A mutations such as the KAT6A knockout mouse that resulted in embryonic lethality due to a failure of hematopoiesis [14]. A knock-in pathogenic variant that eliminates the KAT6A's acetyltransferase function in embryonic stem cells and mouse lines showed proliferation defects, decreased body weight, and decreased life span [14]. Tissue- or cell-specific knockout has shown that KAT6A regulates developmental programs involved in hematopoiesis, skeletogenesis, and thymic and splenic function [14-16]. Further studies demonstrated that KAT6A-mediated acetylation induces the generation of memory B-cell and the CD8 T-cell response to viral infection [17,18]. In addition, transcriptomic profiles of human fibroblast cell lines derived from patients harboring heterozygous KAT6A truncating pathogenic variants demonstrated altered expression of p53-associated genes [3].

At present, fibroblasts cell cultures derived from patients are useful cellular models for understanding the molecular alterations and the response of particular mutations to specific treatments [19]. Thus, biochemical and cellular studies of fibroblasts derived from patients with neurological and neurodevelopmental diseases have provided a lot of useful information on the molecular mechanisms of these disorders [20-24]. The justification for this strategy is based on the hypothesis that, although neurological and neurodevelopmental genetic diseases are primarily located within the central nervous system, patient derived fibroblasts harbor the particular mutation and can reproduce many of the molecular alterations observed within the central nervous system.

In this manuscript, we evaluated the expression levels of proteins involved in acetylation-deacetylation reactions, coenzyme A (CoA) metabolism, mitochondrial proteins, iron metabolism, and antioxidant enzymes in cellular models derived from three KAT6A patients. In addition, we evaluated the effect of epigenetic modulators and mitochondrial boosting agents such as pantothenate and L-carnitine on transcriptome profile, protein expression levels and cell bioenergetics.

2. Materials and Methods

2.1. Reagents

Sodium pantothenate (17288) was purchased from Cayman Chemicals (Michigan). Anti-divalent metal transporter 1 (DMT1) (ABS983), Fetal Bovine Serum (FBS) (F7524),

 doi:10.20944/preprints202211.0273.v1

Oligomycin A (75351-5MG) and Prussian blue (03899-25g) were purchased from Sigma Chemical Co. (St. Louis, MO). was purchased from Invitrogen/Molecular Probes (Eugene, OR). DAPI (sc-3598), L-carnitine (sc-205727), Carbonyl cyanide 4-(trifluoromethoxy) phenylhydrazone (FCCP) (sc-203578), Antimycin A (sc-202467A), Paraformaldehyde (sc-253236), Rotenone (sc-203242), anti-superoxide dismutase 1 (SOD1) (sc-101523), anti-ferritin light chain (sc-74513), were purchased from Santa Cruz Biotechnology (Santa Cruz, CA). Histone H3 Total Acetylation Detection Fast Kit (Colorimetric) (ab115124), NAD/NADH Assay Kit (ab65348), anti-nuclear receptor coactivator 4 (NCOA4/ARA70) (ab86707), anti-sirtuin 1 (SIRT1) (ab110304), anti-Voltage-dependent anion channel 1 (VDAC1) (ab14734), anti-ATP5F1A (ab14748), anti-Nitrogen fixation 1 (NFS1) (ab58623), superoxide dismutase 2 (SOD2) (ab68155), anti-cytochrome C oxidase subunit 4 (COX4) (ab14744), anti-nicotinamide phosphoribosyltransferase 1 (NAMPT1) (ab236874) and anti-mitochondrial ferritin (ab124889) were purchased from Abcam (Cambridge, UK). Dulbecco's Modified Eagle Medium (DMEM) (10524684), Dulbecco's Modified Eagle Medium without glucose (DMEM) (11966025), Penicillin-Streptomycin (11548876), MitoTracker™ Deep Red FM (M22426), anti-pantothenate kinase 2 (PANK2) (CF501355), anti-lysine acetyltransferase 6A (KAT6A/MOZ) (PA568046), anti-glutathione peroxidase 4 (GPX4) (MA5-32827), anti-mitochondrial acyl carrier protein (mtACP) (PA5-30099), anti-sirtuin 3 (SIRT3) (PA5-13222), anti-aminoadipate semialdehyde dehydrogenase phosphopantetheinyl transferase (AASDHPPT) (PA5-39222), anti-NADH: ubiquinone oxidoreductase subunit A9 (NDUFA9) (459100), anti-Iron-sulfur cluster assembly enzyme (ISCU) (MA5-26595), anti-mitoferrin 2 (PA5-42498) and anti-transferrin receptor (TfR) (13-6800) and trypsin (15090-046) were purchased from Thermo-Fisher Scientific (Waltham, MA). Anti-lipoic acid (437695-100UL) was acquired from Merck Millipore (Darmstadt, Germany). Anti-lysine acetylated (9441) was purchased from Cell Signaling Technology (Danvers, MA). Anti-β actin (MBS448085), anti-mitochondrially encoded NADH: ubiquinone oxidoreductase core subunit 6 (MT-ND6) (MBS8518686) and anti-H3K9/K14 acetylated (MBS840797) were purchased from MyBioSource (San Diego, CA). A cocktail of protease inhibitors (complete cocktail) (5892970001) was purchased from Boehringer Mannheim (Indianapolis, IN). Anti- Frataxin (FXN) (LS-C755462) was purchased from LS Bio (Seattle, WA). Takara PCR Mycoplasma Detection Set (6691) was purchased from Clontech. Plasmocure™ - Mycoplasma Elimination Reagent (ant-pc) was purchased from InvivoGen. Agilent Seahorse XF Base Medium (102353-100) and Seahorse XFe24 FluxPak (102340-100) were purchased from Agilent (Santa Clara, CA).

2.2. Ethical statements

Approval of the ethical committee of the Hospital Universitario Virgen Macarena y Virgen de Rocío de Sevilla (Spain) was obtained, according to the principles of the Declaration of Helsinki as well as the International Conferences on Harmonization and Good Clinical Practice Guidelines.

2.3. Cell culture

We used primary skin fibroblast from two healthy subjects (Control 1 and 2) purchased from American Type Culture Collection (ATCC) and three patients harboring KAT6A mutations. One of the patients (P1) has a heterozygous mutation c. [3427-3428 ins TA] that causes a frameshift (p. Ser1143Leu) resulting in a premature stop codon which is predicted to be pathological by prediction tools such as PolyPhen2 [25]. The second patient (P2) is heterozygous carrier of a change in position c. [1075 G>A] (p. Gly359Ser) resulting in an amino acid change in the acetyltransferases domain which likely cause a loss of function. The third patient (P3) carries a heterozygous mutation c. [3385 C>T] causing a premature stop codon (p. Arg1129*). Fibroblast were grown in Dulbecco's Modified Eagle Medium (DMEM- Sigma) supplemented with 10% fetal bovine serum (FBS-Sigma), 100 mg/ml streptomycin, 100U/ml penicillin and 4 mM l-glutamine (Sigma). All the experiments were performed with fibroblasts cell cultures with a passage number <8. Cell

 doi:10.20944/preprints202211.0273.v1

cultures were cleaned from mycoplasma with Plasmocure™-Mycoplasma Elimination Reagent and tested using Takara PCR Mycoplasma Detection Set.

2.4. Immunoblotting

Western blotting was performed using standard methods described in previous manuscripts of the research group [26]. Membranes were incubated with primary antibodies diluted between 1:500 and 1:1000 overnight. Then, the membranes were incubated with the corresponding secondary antibody coupled to horseradish peroxidase at a 1:10000 dilution. The specific proteins were recognized using the Immun Star HRP substrate kit (Biorad Laboratories Inc., Hercules, CA, USA).

Protein loading was assessed by actin expression levels. If the molecular weight of proteins did not interfere, membranes were re-probed with different antibodies. In the event of proteins with different molecular weights, membranes were cut and incubated with specific antibodies. Three biological replicates were used per immunoblot.

2.5. Drug screening

Drugs screenings were performed in nutritional stress medium with galactose as main carbon source. This medium deprives cells from glycolysis as energy source and thus make them rely exclusively in the mitochondrial electron transport chain for adenosine triphosphate (ATP) production [27,28]. In addition, mitochondrial ATP production was slightly impaired with oligomycin at low concentration (0.5 nM). In this medium, mutant KAT6A fibroblasts were unable to survive.

Fibroblasts were cultured in DMEM and treated for 15 days with several compounds at different concentrations. Nutritional stress medium was prepared with DMEM without glucose, 10 mM galactose, 0.5 nM oligomycin, 1% of antibiotic solution and 10% FBS. First, fibroblasts were seeded in 24-well plates in DMEM. After 24h cells were treated again for 72 h with the same compound at the same concentration. Then the cell culture medium was removed, and cells were cultured in stress medium (Time 0). Thereafter, the treatments were re-applied at the same concentration. The 72 hours endpoint was selected because cells showed a significant cell proliferation/death at this time. Cell viability was tested by live cell imaging counting and trypan blue 0.2% staining. Cell counting was acquired using the BioTek™ Cytation™ 1 Cell Imaging Multi-Mode Reader (BioTek, Winooski, VT, United States). Each drug screening was performed in three biological replicates.

2.6. Immunofluorescence microscopy

Immunofluorescence studies were performed using a protocol previously described by our research group [29]. Cells were cultured on 1 mm width (Goldseal No.1) glass coverslips for 24 to 48 hours in DMEM with 20% FBS. Cells were washed once with Phosphate Buffered Saline (PBS), fixed in 3,8% paraformaldehyde in 0,1% of saponin for 5 minutes. For immunostaining, glass coverslips were incubated with primary antibodies diluted 1:100 in PBS, 1–2 hours at 37 °C in a humidified chamber. The excess of antibodies were removed by washing with PBS (three times during 5 minutes). Then, secondary antibodies diluted in 1:1000 in PBS, were added and incubated for 1 hour at 37ºC. Coverslips were then rinsed with PBS for 3 minutes, incubated for 1 minute with PBS containing Hoechst 33,342 (1µg/ml) and washed with PBS (3 times, 5 minutes). Finally, coverslips were mounted onto microscope slides using Vectashield Mounting Medium (Vector Laboratories, Burlingame, CA, USA) and analyzed using an upright fluorescence microscope (Leica DMRE, Leica Microsystems GmbH, Wetzlar, Germany). Each immunofluorescence assay was performed in three biological replicates.

2.7. RNAseq

Fibroblasts were cultured until confluence. Then, cells were tested for mycoplasma by PCR and cellular pellets were obtained. RNA was extracted and purified using RNeasy Mini Kit (QIAGEN, Hilden, Germany). DNase digestion was performed with the RNase-

 doi:10.20944/preprints202211.0273.v1

Free DNase Set (QIAGEN, Hilden, Germany). RNAseq was performed by Microomics Systems S.L. (Barcelona, Spain).

Libraries were prepared using the TruSeq stranded mRNA Library Prep (96 samples ref. 20020595 or 48 samples ref. 20020594) according to the manufacturer's protocol, to convert total RNA into a library of template molecules of known strand origin and suitable for subsequent cluster generation and DNA sequencing.

Briefly, 1000 or 500 ng of total RNA were used for poly(A)-mRNA selection using poly-T oligo attached magnetic beads using two rounds of purification. During the second elution of the poly-A RNA, the RNA was fragmented under elevated temperature and primed with random hexamers for cDNA synthesis. Then, the cleaved RNA fragments were copied into first strand cDNA using reverse transcriptase (SuperScript II, ref. 18064-014, Invitrogen) and random primers. After that, second strand cDNA was synthesized, removing the RNA template and synthesizing a replacement strand, incorporating dUTP in place of dTTP to generate ds cDNA using DNA Polymerase I and RNase H.

These cDNA fragments, then had the addition of a single 'A' base to the 3'ends of the blunt fragments to prevent them from ligating to one another during the adapter ligation. A corresponding single T nucleotide on the 3' end of the adapter provides a complementary overhang for ligating the adapter to the fragments. Subsequent ligation of the multiple indexing adapter to the ends of the ds cDNA was done. Finally, PCR selectively enriched those DNA fragments that had adapter molecules on both ends. The PCR was performed with a PCR Primer Cocktail that anneals to the ends of the adapters.

Final libraries were analyzed using Bioanalyzer DNA 1000 or Fragment Analyzer Standard Sensitivity (ref: 5067-1504 or ref: DNF-473, Agilent) to estimate the quantity and validate the size distribution. Libraries were then quantified by qPCR using the KAPA Library Quantification Kit KK4835 (REF. 07960204001, Roche) prior to the amplification with Illumina's cBot. Libraries were sequenced with 125-bp paired-end reads on Illumina's HiSeq2500.

Sequencing coverage is around 25 million reads. Raw demultiplexed forward and reverse reads were processed using the following steps: Reads quality control of RNA with FastQC v.0.11.8 have a Phred-Score (Q) greater than 30 (Figure S15) and Pre-processing with Trimmomatic v0.39 [30]. The primary processing were processed using the following steps: Alignment to genome reference Homo_sapiens.CRGh38.102 from Ensembl using Bowtie2 v 2.3.5.1 [31], Alignment quality control with qualjmap v.2.2.2 [32], counts table with featureCounts v1.6.4 [33] and differential expression analysis with DeSeq2 v1.24.0 [34]. Genes differentially expressed have Pvalue<0.05 and log2FoldChange negative between -13.89 and -0.048 and positive between 0.043 and 13.24. Enrichment Scores were calculated using Merico et al. 2010 methods [35].

2.8. Cell fractioning

Cells were cultured until confluence; cell pellets were homogenized using a fractionation buffer that contains 250 mM sucrose, 10 mM Tris, 1 mM ethylene diamine tetra acetate (EDTA) and proteases inhibitors cocktail, pH 7.4. Cell suspension was passed through a 25-gauge needle 8 times using a 1 mL syringe. Next, nuclei and intact cells were removed by centrifugation at 1500 g for 20 minutes. Supernatant with intact mitochondria was transferred into a new tube and centrifuged at 12000 g for 10 minutes (pellet at the bottom – "mitochondria fraction". Supernatant – "cytosolic fraction"). Supernatant was transferred into another new tube. Cytosolic fractions were concentrated using Centricon YM-10 devices (Millipore) according to the manufacturer`s instructions.

2.9. Bioenergetics

Mitochondrial respiratory function of control and mutant KAT6A fibroblasts were measured using a mito-stress test assay with an XF24 extracellular flux analyzer (Seahorse Bioscience, Billerica, MA, United States, 102340-100) according to the manufacturer´s instructions and previous studies [36,37]. Fibroblasts were seeded at a density of $1{,}5x10^4$

 doi:10.20944/preprints202211.0273.v1

cells/well with 500 µL of growth medium (DMEM medium containing 20% of FBS) in XF24 cell culture plates and incubated for 24 h at 37ºC and 5% of CO_2. Subsequently, growth medium was removed from the wells, leaving on them only 50 µl medium. Then, cells were washed twice with 500 µl of pre-warmed assay XF base medium (102353-100) supplemented with 10mM glucose (103577-100), 1 mM glutamine (103579-100) and 1 mM sodium pyruvate (103578-100); pH 7.4) and eventually 450 µl of assay medium (500 µl final) were added. Cells were incubated at 37°C without CO_2 for 1 h to allow pre-equilibrating with the assay medium. Mitochondrial functionality was evaluated by sequential injection of four compounds affecting bioenergetics. The final concentrations of the injected reagents were: 1 µM oligomycin, 2 µM carbonyl cyanide 4-(trifluoromethoxy) phenylhydrazone (FCCP), 1 and 2.5 µM rotenone/antimycin A. The best concentration of each inhibitor and uncoupler, as well as the optimal cells seeding density were determined in preliminary analyses. A minimum of five wells per treatment were used in each experiment. This assay allowed for an estimation of basal respiration, maximal respiration and spare respiratory capacity.

2.10. NAD^+/NADH Levels

Nicotinamide adenine dinucleotide (NAD^+/NADH) levels in cellular pellets were assessed by the NAD^+/NADH Colorimetric Assay Kit (Abcam, Hercules, CA, United States, ab65348) protocol. Absorbance was measured using a POLARstar Omega plate reader (BMG Labtech, Offenburg, Germany). Each assay was performed in three biological replicates.

2.11. Histone H3 total acetylation

Histone H3 total acetylation levels in cellular pellets were assessed by the Histone H3 Total Acetylation Colorimetric Detection Fast Kit (Abcam, Hercules, CA, United States, ab115124) protocol. Absorbance was measured using a POLARstar Omega plate reader (BMG Labtech, Offenburg, Germany). Each assay was performed in three biological replicates.*2.13.*

2.12. Statistical analyses

Statistical analyses were performed as formally described by our research group [38]. We used without any distributional assumption non-parametric statistics when number of events was small (n<30) [39]. In this cases, multiple groups were compared using a Kruskal-Walli test. In case of only two groups, they were compared using the method of Mann-Whitney test. On the other hand, when the events were higher (n>30), we used parametric tests. Cases with multiple groups were compared using a one-way ANOVA. After this comparison we applied Bonferroni post-hoc test for looking for significant differences between groups. When we have two groups, they were compared applying a student´s t-test with a Welch´s correction. Statistical analyses were leaded applying the GraphPad Prism 7.0 (GraphPad Software, San Diego, CA). The data are reported as representative of at least three independent experiments. P-values of less than 0.05 were considered significant.

3. Results

3.1. Protein expression levels in KAT6A fibroblasts

3.1.1. Expression levels of KAT6A enzyme are markedly reduced in fibroblasts derived from KAT6A patients

First, we analyzed protein expression levels of the mutant KAT6A enzyme in fibroblast cell lines derived from three KAT6A patients and two healthy subjects (C1 and C2). The three patients have heterozygous mutations in the *KAT6A* gene. Patient 1 (P1) has an insertion of two amino acids that results in a premature stop codon; patient 2 (P2) has a base change; and the patient 3 (P3) has a base change that results in a premature stop

Preprints (www.preprints.org) | NOT PEER-REVIEWED | Posted: 15 November 2022 doi:10.20944/preprints202211.0273.v1

codon. KAT6A protein expression levels were markedly reduced in the three patient cell lines (Figure 1A and Figure S1A). Curiously, KAT6A expression levels were higher in P2 fibroblasts than P1 and P3 fibroblasts suggesting that the expression levels of the mutant enzyme may depend on the type of mutation. In addition, SIRT1 and SIRT3 (Sirtuins 1 and 3), nicotinamide adenine dinucleotide (NAD^+)-dependent protein deacetylases, as well as NAMT (Nicotinamide phosphoribosyltransferase), the rate-limiting enzyme in the NAD^+ salvage pathway, were also downregulated in mutant cells (Figure 1A and Figure S1A). These results suggest that KAT6A mutations lead to downregulation of enzymes involved in both acetylation and deacetylation processes.

3.1.2. Expression of proteins involved in coenzyme A (CoA) metabolism were also affected in mutant KAT6A fibroblasts

As KAT6A enzyme uses acetyl-CoA as substrate for histones acetylation, we next addressed the expression levels of proteins implicated in CoA metabolism and downstream proteins such as mtACP (mitochondrial acyl carrier protein), mitochondrial lipoylated proteins and AASDHPPT (aminoadipate-Semialdehyde Dehydrogenase-Phosphopantetheinyl Transferase), and enzyme involved in the hydrolysis of CoA and the transfer of the 4′-phosphopantetheinyl moiety to mitochondrial proteins such as mtACP [40,41]. Expression levels of pantothenate kinase 2 (PANK2), mtACP, lipoylated PDH (pyruvate dehydrogenase), lipoylated KGDH (α-ketoglutarate dehydrogenase) and AASDHPPT were markedly reduced in mutant KAT6A fibroblasts (Figure 1B and Figure S1B). These results suggest that proteins involved in CoA biosynthesis and downstream CoA-dependent pathways are downregulated in mutant KAT6A fibroblasts.

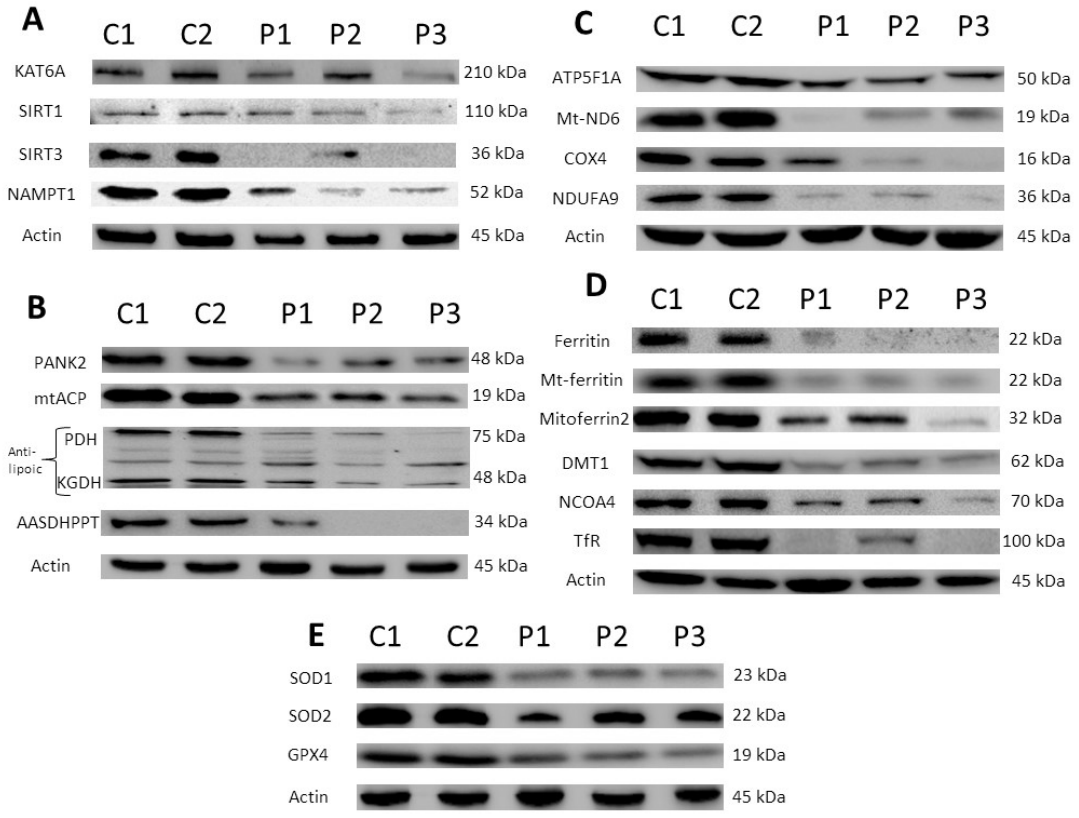

Figure 1. Protein expression patterns in control and KAT6A mutant fibroblasts. Protein extracts of Control (C1 and C2) and patient (P1, P2 and P3) cell lines were separated on a SDS polyacrylamide gel and immunostained with primary antibodies (A) Proteins related to acetylation-deacetylation reactions: KAT6A, SIRT1, SIRT3 and NAMPT1, (B) proteins related to CoA metabolism: PANK2, mtACP, lipoylated PDH, lipoylated KGDH, AASDHPPT. (C) mitochondrial proteins: ATP Syntase, Mt-NAD6, COX4 subunit, NDUFA9 (D) proteins related to iron metabolism: Ferritin, Mt-ferritin,

 doi:10.20944/preprints202211.0273.v1

Mitoferrin 2, DMT1; NCOA4, TfR. (E) antioxidant enzymes: . A representative actin lane is shown, although loading control was additionally checked for every Western blot. Data represent the mean ±SD of three separate experiments. Quantification of protein bands using densitometry is shown in Supplementary Figure S1-2.

3.1.3. Expression levels of mitochondrial respiratory chain proteins were affected in KAT6A mutant fibroblasts.

To characterize the pathological consequences of KAT6A deficiency in patient derived fibroblasts, we next examined the expression levels of proteins involved in mitochondrial respiratory chain. Expression levels of several mitochondrial subunits such as NDUFA9, COX4, Mt-ND6 and ATP5F1A were notably reduced in KAT6A fibroblasts (Figure 1C and Figure S1C). In contrast, expression levels of VDAC1, a marker of mitochondrial content of cells [42], were not affected (Figure S3C and S3D). These results suggest that there is a down-regulation of several essential mitochondrial proteins in KAT6A fibroblasts. The decreased levels of essential mitochondrial proteins may lead to mitochondrial dysfunction, increased reactive oxygen species (ROS) production and reduced energy generation.

3.1.4. Expression levels of several proteins implicated in iron metabolism were reduced in mutant KAT6A fibroblasts.

As PANK2 and mtACP deficiency may alter iron metabolism [40], we then explored the expression levels of several proteins involved in iron handling. As displayed in Figure 1D and Figure S2A, expression levels of several proteins related to this pathway are reduced such as Transferrin receptor (TfR), DMT1, ferritin, mitoferrin2, mitochondrial ferritin and NCOA4, were markedly reduced in mutant KAT6A fibroblasts. However, the expression levels of proteins involved in iron-sulfur clusters biosynthesis such as ISCU (Iron-sulfur cluster assembly enzyme), NFS1 (NFS1 cysteine desulfurase) and FXN (Frataxin) were not affected. In addition, intracellular iron accumulation assessed by Prussian blue staining was not observed in mutant KAT6A fibroblasts (Figure S3).

3.1.5. Expression levels of antioxidant enzymes were also reduced in mutant KAT6A fibroblasts.

As mitochondrial dysfunction can increase oxidative stress, we also addressed protein expression levels of antioxidant enzymes. Protein expression levels of SOD1, SOD2 and GPX4 were markedly reduced in mutant KAT6A fibroblasts (Figure 1E and Figure S2B). These results indicate that the enzymatic antioxidant system is downregulated in mutant KAT6A fibroblasts.

3.2. Effect of pantothenate on KAT6A fibroblasts

3.2.1. Pantothenate and L-carnitine supplementation enhance survival of the mutant KAT6A fibroblasts in nutritional stress medium.

As mitochondrial dysfunction can be a critical pathological feature in mutant KAT6A fibroblasts, we developed a screening protocol in nutritional stress medium to force mitochondrial function and induce cell death in mutant fibroblasts. In these conditions, cell survival rescue by pharmacological compounds is an interesting approach for the identification of supplements capable of correcting the mutant phenotype. Thus, control and mutant P1 fibroblasts were cultured for 15 days on glucose rich DMEM medium without or with supplements at different concentrations. Then, the medium was replaced by galactose medium with 0.5 nM of oligomycin. As expected, no differences could be observed on the cell proliferation in control fibroblasts (Figure 2A-B). In contrast, KAT6A fibroblasts did not survive in stress medium (Figure 2C-D and Figure S4-6). Curiously, supplementation with 0.8 μM of pantothenate, a CoA metabolism activator, or 0.8 μM of L-carnitine, a mitochondrial boosting agent, enabled the survival of mutant KAT6A fibroblasts in stress medium (Figure 2E-H and Figure S4-6), although the cell proliferation was slower

Preprints (www.preprints.org) | NOT PEER-REVIEWED | Posted: 15 November 2022 doi:10.20944/preprints202211.0273.v1

than in normal medium. Interestingly, the combined treatment with pantothenate and L-carnitine showed a synergic positive effect in cell survival. In addition, KAT6A cells survived at lower concentration of pantothenate and L-carnitine (Figure 2I-J and Figure S4-6).

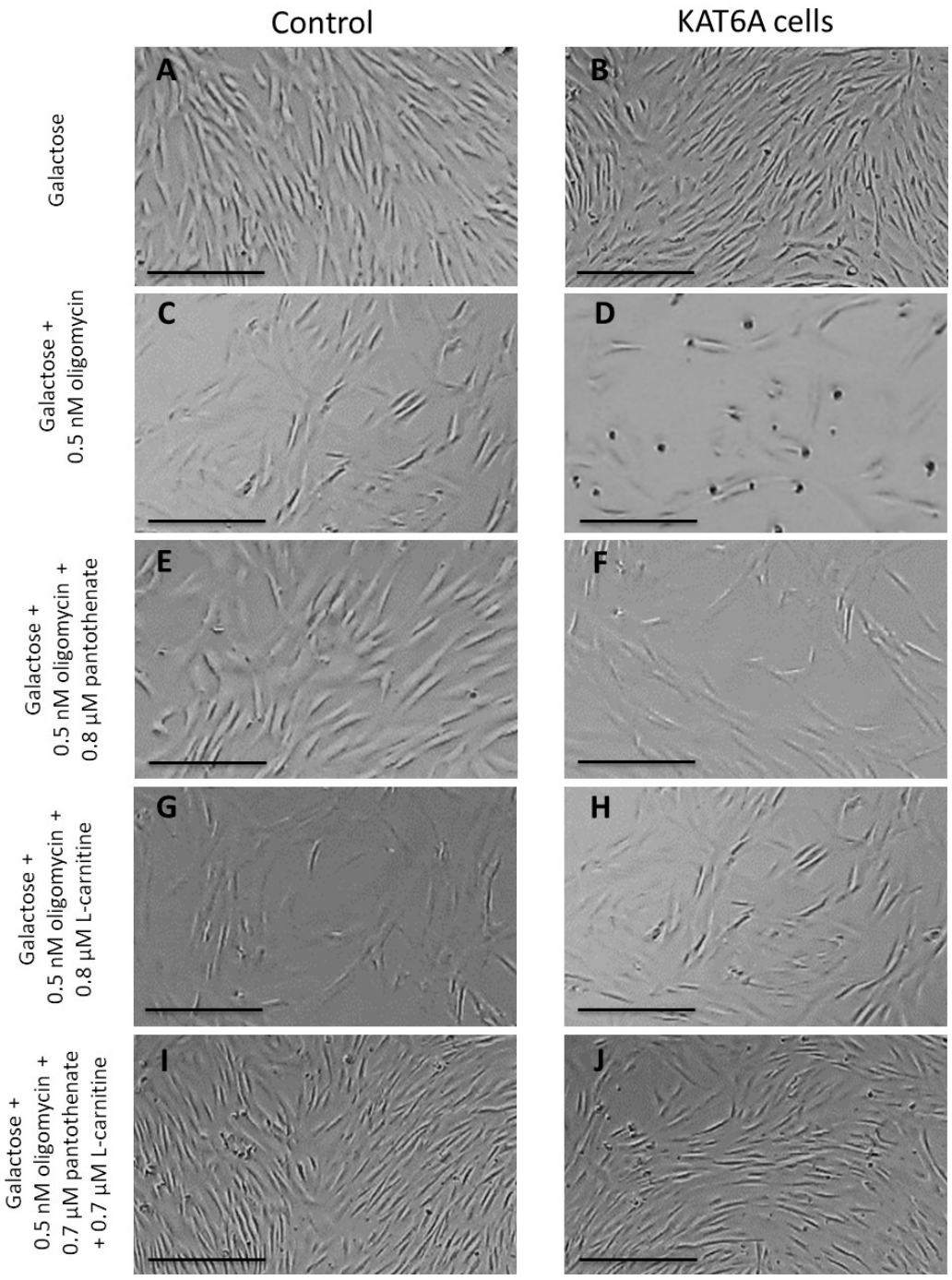

Figure 2. Survival screening assays in galactose medium. Control (C1) and mutant KAT6A fibroblasts (P1) were initially cultured in DMEM high glucose. After 3 days, glucose medium was changed to galactose medium with 0.5 nM oligomycin. Images were acquired right after changing the medium and after 72 h of incubation. (A-B) Control and mutant KAT6A fibroblasts in glucose medium. (C-D) Control and mutant KAT6A fibroblasts in stress medium. (E-F) Control and mutant KAT6A fibroblasts (P1) treated with 0.8 µM pantothenate in stress medium. (G-H) Control and mutant KAT6A fibroblasts treated with 0.8 µM L-carnitine in stress medium. (I-J) Control and mutant KAT6A fibroblasts (P1) treated with 0.7 µM pantothenate and 0.7 µM L-carnitine in stress medium.

 doi:10.20944/preprints202211.0273.v1

Data represent the mean ±SD of three separate experiments. The quantification of cellular proliferation rate is shown in Supplementary Figure S4-6. Scale bar= 200 μm.

The lowest concentrations of pantothenate and L-carnitine necessary for cell survival in stress medium varied among the different KAT6A cell lines suggesting that KAT6A mutations may response differently to pantothenate and L-carnitine concentrations (Figure S4-6). We found that patient 1 and patient 3 cells survived at 0.7 μM of pantothenate and 0.7 μM of L-carnitine, while patient 2 cells survived at 0.4 μM of pantothenate and 0.4 μM of L-carnitine.

3.2.2. Pantothenate and L-carnitine supplementation corrects partially or totally protein expression patterns in mutant KAT6A cell lines.

Next, we assessed the positive effect of pantothenate and L-carnitine supplementation on the expression levels of mutant KAT6A enzyme, SIRT1, SIRT3, NAMPT, mitochondrial proteins (Mt-ND6 and NDUFA9), CoA metabolism-related proteins (PANK2, mtACP, lipoylated PDH and lipoylated KGDH), and antioxidant enzymes (SOD1, SOD2 and GPX4). The expression levels of these proteins were markedly downregulated in the three KAT6A cell lines, although to different extents due to the broad diversity in genetic backgrounds and type of mutations. Interestingly, treatment with pantothenate and L-carnitine enhanced the expression levels of all down-regulated proteins (Figure 3 and Figure S7-8). Different concentrations of pantothenate and L-carnitine were used in the mutant cell lines according to the minimum concentration required for survival in the screening assay in stress medium. Patient 1 and patient 3 were treated with 0.7 μM L-carnitine and 0.7 μM pantothenate (Figure 3A, C and Figure S7-8), while patient 2 was treated with 0.4 μM L-carnitine and 0.4 μM pantothenate (Figure 3B and Figure S7-8).

Preprints (www.preprints.org) | NOT PEER-REVIEWED | Posted: 15 November 2022 doi:10.20944/preprints202211.0273.v1

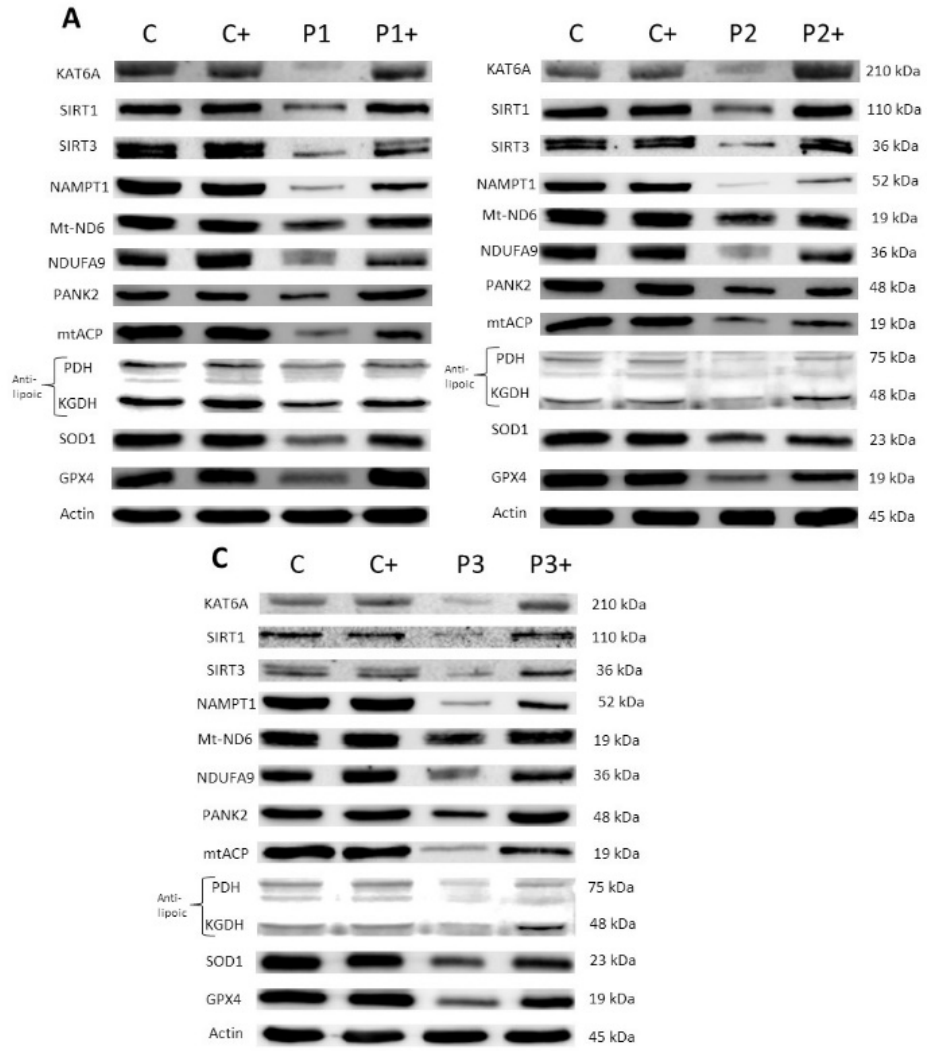

Figure 3. Effect of pantothenate and L-carnitine supplementation on protein expression patterns in control and mutant KAT6A fibroblasts. Control (C+) and mutant P1 and P3 fibroblasts (P1+ and P3+) were treated with 0.7 μM pantothenate and 0.7 μM L-carnitine for 15 days. P2 fibroblasts (P2) were treated with 0.4 μM pantothenate and 0.4 μM L-carnitine for 15 days. Immunoblotting analysis of cellular extracts from control and P1 fibroblasts (A), P2 fibroblasts (B) and P3 fibroblasts (C). Protein extracts were separated on a SDS polyacrylamide gel (12,5%) and immunostained with antibodies against KAT6A protein, SIRT1, SIRT3, NAMPT1, Mt-ND6, NDUFA9, PANK2, mtACP, lipoic acid (lipoylated PDH and lipoylated KGDH), SOD1, GPX4 and actin. A representative actin band is shown, although loading control was additionally checked for every Western blot. Data represent the mean±SD of three separate experiments. Protein band densitometry is shown in Supplementary Figure S7-8.

3.2.3. Pantothenate and L-carnitine supplementation increases histones acetylation in KAT6A cells.

As KAT6A enzyme acetylates lysine 9 and lysine 14 of histone H3, we next assessed the efficacy of pantothenate and L-carnitine in improving acetylation activity. For this purpose, total acetylation of histone H3 were determined in control and mutant KAT6A P1 fibroblasts by immunofluorescence and a colorimetric assay in nuclear fractions. Histone acetylation of mutant KAT6A fibroblasts was significantly reduced in mutant KAT 6A fibroblasts (Figure 4A-B and Figure S9). Interestingly, the supplementation of mutant cells with pantothenate and L-carnitine induced a marked increase in histone acetylation reaching levels similar to those of control cells (Figure 4A-B and Figure S9). These findings suggest that histone acetylation deficiency in KAT6A fibroblasts was corrected by pantothenate and L-carnitine supplementation. The positive effect of pantothenate and L-

Preprints (www.preprints.org) | NOT PEER-REVIEWED | Posted: 15 November 2022 doi:10.20944/preprints202211.0273.v1

carnitine on histone acetylation was also confirmed in P2 and P3 mutant cell lines (Supplementary Figures S10-S11).

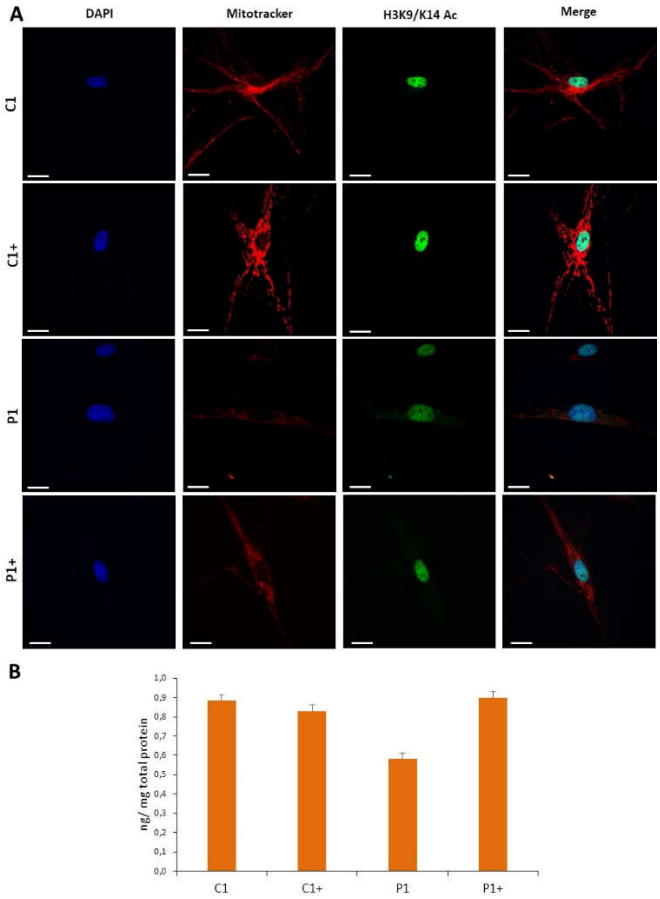

Figure 4. Effect of 0.7 μM pantothenate and 0.7 μM L-carnitine on histone acetylation levels in control (C) and KAT6A fibroblasts (P1). Control (C+) and mutant P1 fibroblasts (P1+) were treated with 0.7 μM pantothenate and 0.7 μM L-carnitine for 15 days. (A) Control and KAT6A fibroblasts were incubated with Mitotracker DeepRed FM 100 nM for 45 min, then they were fixed and immunostained with anti-H3K9/K14 and examined by fluorescence microscopy. Fifty cells per condition were analyzed. (B) Histone H3 total acetylation levels in cellular pellets were assessed by the Histone H3 Total Acetylation Colorimetric Detection Fast Kit (Abcam, Hercules, CA, United States, ab115124) protocol. Data represent the mean ±SD of three separate experiments. Absorbance was measured using a POLARstar Omega plate reader (BMG Labtech, Offenburg, Germany). The mitotracker DeepRed and H3K9/K14 intensity assessment were performed using FIJI software and it is shown in Supplementary Figure S9. *p-value < 0.05 and **p-value < 0.01. Scale bar= 15 μm. C+ and P1+, treated control and P1 cell lines, respectively.

Next, we measured NAD total (NADt), NAD^+, NADH levels and the NAD^+/NADH ratio, since they are sirtuins cofactors involved in histone deacetylation reactions by SIRTs (Figures 5A, 5B, 5C, and 5D). Our results showed that NADt, NAD^+, NADH content and the NAD+/NADH ratio were significantly reduced in KAT6A mutant cells, and that pantothenate and L-carnitine treatment was able to correct their intracellular levels. These findings suggest that pantothenate and L-carnitine treatment also correct the content of NAD^+ that is essential cofactor for sirtuins' function and histone deacetylation reactions.

 doi:10.20944/preprints202211.0273.v1

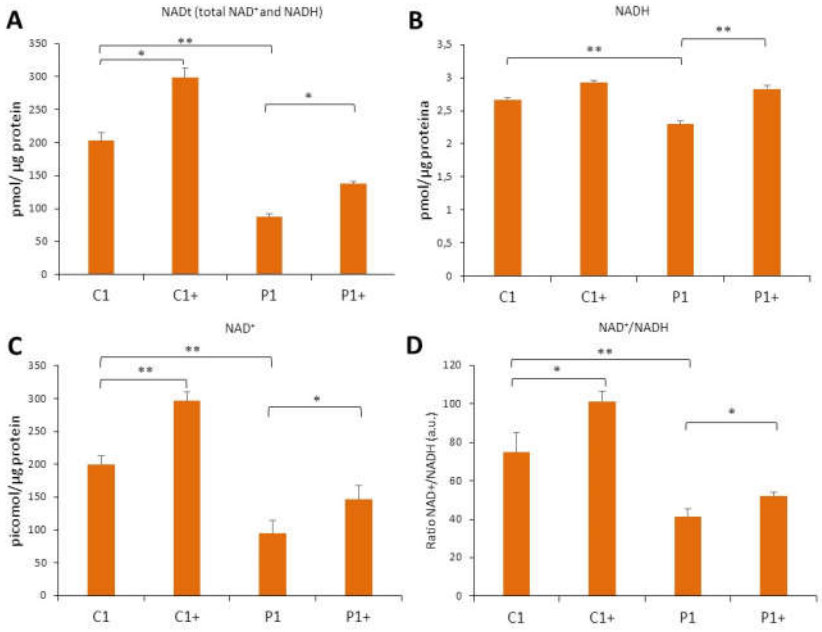

Figure 5. Effect of 0.7 µM pantothenate and 0.7 µM L-carnitine on cellular NAD+/NADH levels in control (C) and KAT6A mutant fibroblasts (Patient 1 – P1). Control (C+) and KAT6A fibroblasts (P1+) were treated for 15 days with 0.7 µM pantothenate and 0.7 µM L-carnitine. NAD+/NADH assay was performed using the NAD+/NADH Assay Kit. NADt (total NAD+ and NADH) (A) and NADH (B) were quantified as descibed in material and methods. NAD+ was calculated by subtraction (NADt – NADH) (C) and NAD+/NADH ratio by the equation ((NADt-NADH)/NADH (D). Data represent the mean ±SD of three separate experiments. *p-value < 0.05 and **p-value < 0.01.

3.2.4. Pantothenate and L-carnitine supplementation improves cell bioenergetics in KAT6A mutant fibroblasts.

To test the efficacy of pantothenate and L-carnitine treatment in improving mitochondrial activity, we assessed mitochondrial membrane potential by Mitotracker staining and cell bioenergetics using the XF Cell Mito Stress assay. As expected, mitochondrial bioenergetics was altered in mutant KAT6A fibroblasts presenting a general decrease in mitochondrial membrane potential (Figure 4 and Figure S9) and mitochondrial bioenergetic parameters (Figure 6A-B). Confirming the positive effect previously observed, 0.7 µM pantothenate and 0.7 µM L-carnitine supplementation significantly restored mitochondrial membrane potential (Figure 4 and Figure S9) and mitochondrial maximal respiration and spare respiratory capacity in mutant KAT6A fibroblasts (Figure 6A-B). These results are consistent with the recovery of mitochondrial protein expression levels under supplementation with pantothenate and L-carnitine (Figure 3) and the recovery of mitochondrial membrane potential (Figure 4A and Figure S9). The positive effect of pantothenate and L-carnitine on mitochondrial membrane potential and cell bioenergetics was also confirmed in P2 and P3 mutant cell lines (Supplementary Figures S10-13).

Preprints (www.preprints.org) | NOT PEER-REVIEWED | Posted: 15 November 2022 doi:10.20944/preprints202211.0273.v1

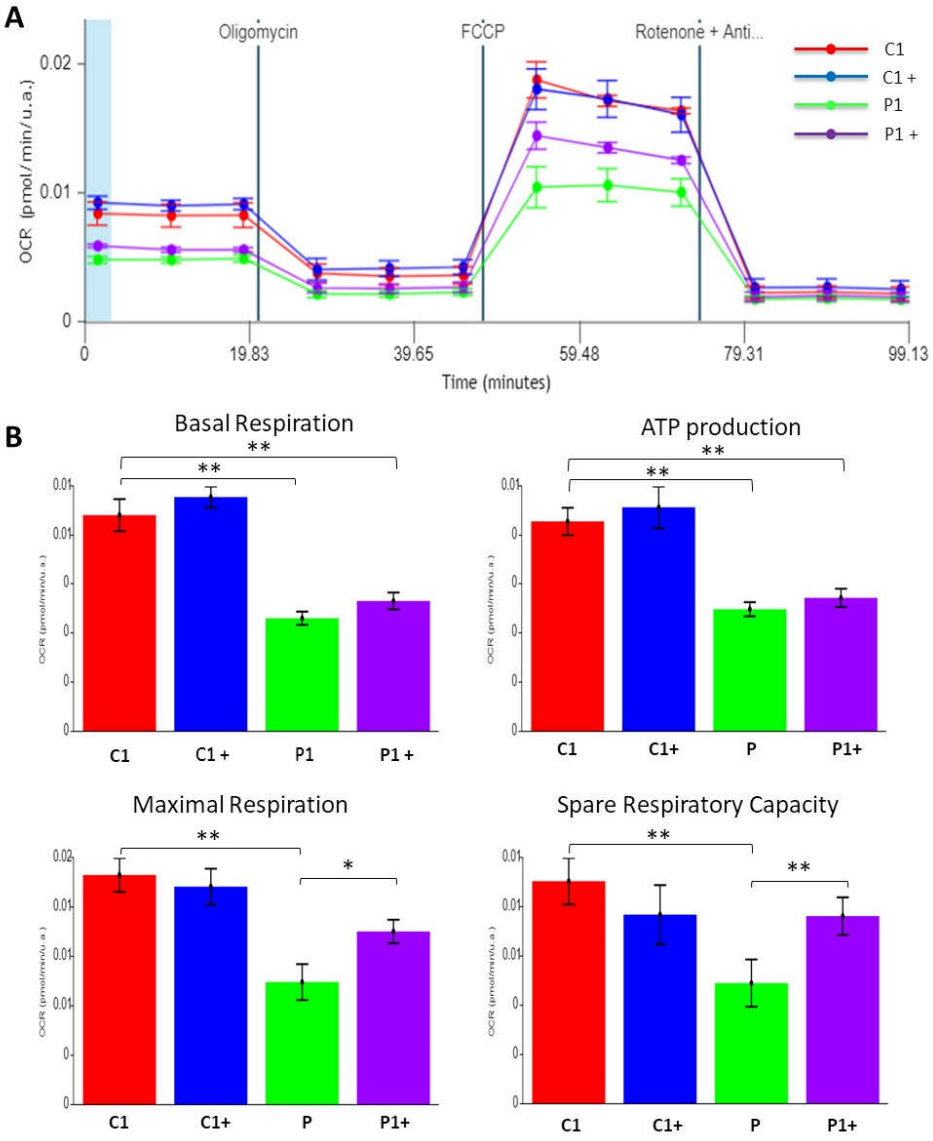

Figure 6. Effect of pantothenate and L-carnitine supplementation on mitostress bioenergetic assay in control (C) and mutant KAT6A fibroblasts (P1). Control (C+) and KAT6A fibroblasts (P1+) were treated for 15 days with 0.7 µM pantothenate and 0.7 µM L-carnitine. (A) Mitochondrial respiration profile was measured with a Seahorse XFe24 analyzer. Fibroblasts were treated for 15 days with 0.7 µM pantothenate and 0.7 µM L-carnitine. (B) Basal respiration, ATP production, maximal respiration and spare respiratory capacity were assessed by Seahorse analytics website. *p-value < 0.05 and **p-value < 0.01.

3.2.5. Pantothenate and L-carnitine treatment highly modifies the transcriptome.

To analyze the pathological effects of KAT6A mutations and to assess the effect of 0.7 µM pantothenate and 0.7 µM L-carnitine supplementation on gene expression, we next performed a RNA-seq (RNA sequencing) analysis on control and mutant KAT6A P1 fibroblasts with and without pantothenate/carnitine treatment. The RNA-seq was meant to give a resulting expression value for each gene and an average of its expression levels across the different conditions. Among the 60675 expressed genes that were detected, 12719 showed differential expression between control and mutant KAT6A fibroblasts, 10026 showed differential expression between mutant KAT6A fibroblasts and treated KAT6A mutant fibroblasts and 11530 showed differential expression between control and treated mutant KAT6A fibroblasts Figure 7A-B, D-E, G-H. Moreover, we assessed the effect of pantothenate and L-carnitine treatment on control fibroblasts. Results showed that only 134 genes were differentially expressed in control cells after treatment.

Preprints (www.preprints.org) | NOT PEER-REVIEWED | Posted: 15 November 2022 doi:10.20944/preprints202211.0273.v1

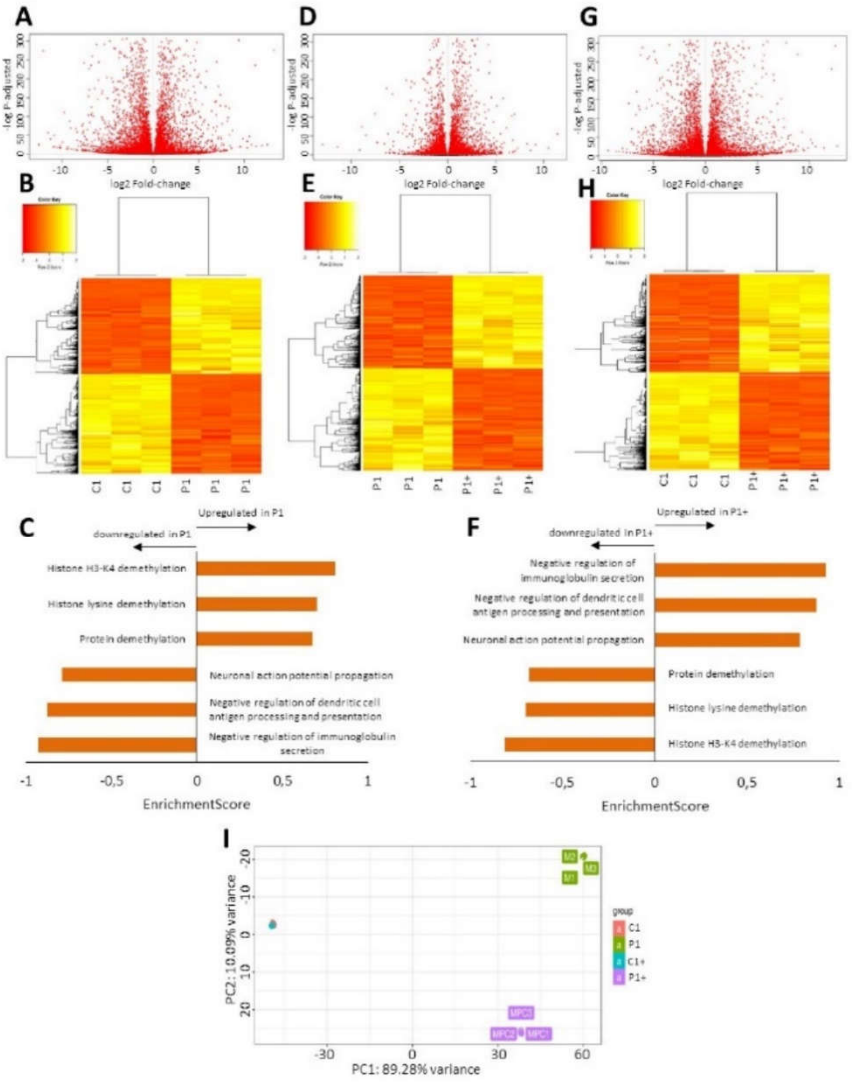

Figure 7. Effect of pantothenate and L-carnitine supplementation on gene expression (RNAseq) in control and mutant KAT6A fibroblasts. Control (C+) and KAT6A fibroblasts (P1+) were treated for 15 days with 0.7 μM pantothenate and 0.7 μM L-carnitine. Volcano plot display the relationship between fold-change and p-values (represented as –log p-adjusted, adj) on the differentiation between control and mutant KAT6A fibroblasts (A), mutant KAT6A and treated mutant KAT6A fibroblasts (D) and control and treated mutant KAT6A fibroblasts (G). Genes differentially expressed with P adj<0.05 are highlighted in red. Heatmap of the relative expression of all differentially expressed genes between control and mutant KAT6A fibroblasts (B), mutant KAT6A and treated mutant KAT6A fibroblasts (E) and control and treated mutant KAT6A fibroblasts (H). To better interpret RNAseq results, genes were annotated using a functional classification scheme: The Biological Process Ontology (BP) which cover gene functions. The results were the comparison between control and mutant KAT6A fibroblasts (C) and mutant KAT6A and treated mutant KAT6A fibroblasts. PCA (Principal Component Analysis) plot is showed to see transcriptomic level differences (I).

Since the human KAT6A protein regulation pathway remains obscure, no databases like the Kyoto Encyclopedia of Genes and Genomes (KEGG) are available to study the proteins involved in it. For this reason, biological process ontology (BP) was used to assess which of the differentially expressed genes might be related with KAT6A protein. BP analysis demonstrated that the genes related to acetylation/methylation were decreased and neuronal regulation genes were increased in mutant KAT6A fibroblasts respect to control fibroblasts (Figure. 7C- 7F). Interestingly, these pathways recover their normal expression pattern under pantothenate and L-carnitine supplementation (Figure. 7F). No significant differences were found between control and treated mutant KAT6A fibroblasts. These

 doi:10.20944/preprints202211.0273.v1

results suggest that there is a recovery on gene expression patterns under pantothenate and L-carnitine supplementation. As we can see in the Figure 7I, the PCA (Principal Component Analysis) plot showed that treated mutant KAT6A fibroblast recover partially the transcriptomic pattern of control cells.

Next, we analyzed the expression changes of specific genes between treated and untreated conditions. We found that the expression levels of down-regulated genes in mutant KAT6A fibroblasts such as *KAT6A*, *SIRT1*, *SIRT3*, *NAMPT1*, *Mt-ND6*, *NDUFA9*, *PANK2*, *mtACP*, *PDH* (*E1 subunit α2*), *KGDH* (*E2 subunit*), *SOD1*, *SOD2* and *GPX4* were significantly restored after pantothenate and L-carnitine treatment (Figure S14). The proteins encoded by these genes are involved in acetylation-deacetylation pathways, CoA metabolism, mitochondria and antioxidant enzymes, all of them critical for intracellular processes in embryonic and childhood development.

4. Discussion

In this study, we assessed the pathophysiological alterations present in three patients-derived fibroblasts cell lines carrying *KAT6A* mutations. Our results suggest that patient-derived fibroblasts are interesting biological models for recreating the pathological alterations of the disease. In addition, cellular models can facilitate the screening of a large number of compounds and evaluate their positive effect on altered pathways.

Our results demonstrated that KAT6A enzyme expression levels were markedly reduced in fibroblasts derived from KAT6A patients. Furthermore, we showed that deficiency of KAT6A reduced histone H3 acetylation and led to altered gene expression patterns and down-regulation of essential proteins in cell metabolism. Screening survival assays in nutritional stress medium identified two positive compounds, pantothenate and L-carnitine. Interestingly, the supplementation with pantothenate and L-carnitine, increased the expression levels of KAT6A mutant enzyme accompanied by a significant correction of histone acetylation and recovery of gene expression patterns and expression levels of affected proteins.

KAT6A (MOZ/ MYST3) is a MYST family transcriptional coactivator with histone acetyltransferase activity [43]. Transcriptional coactivators form multiprotein complexes that are recruited to specific genomic localizations by DNA-binding transcription factors. Coactivator complexes commonly contain an enzyme subunit with chromatin-modifying activity, such as a histone acetyltransferase [44]. It has been suggested that the exchange of a corepressor complex with a coactivator complex having a histone acetyltransferase such as KAT6A, may be an essential process in promoting gene expression [45]. Coregulator complexes determine an additional regulation level where transcriptome and consequently protein expression and cellular phenotype are modulated [46].

KAT6A is essential for fundamental pathways such as hematopoietic stem cells, normal B cell development, cell cycle progression and stem cell self-renewal among others [16,17,47-49]. Thus, dysregulation of these processes due to KAT6A deficiency produces positive and negative expression of proteins involved in these processes as well as in cellular senescence [50,51].

The acetylation status of histones is produced by the opposing action of histone acetyltransferases and histone deacetylases [52]. Histone acetylation is a critical epigenetic modification that changes chromatin architecture and regulates gene expression by opening or closing the chromatin structure [53]. The decrease of KAT6A protein levels alters the acetylation status of histones, and therefore the transcription of many essential genes implicated in critical cellular processes [8,11,12,54-56]. For all these reasons the up regulation of the expression levels of KAT6A can be a critical target for restoring histone acetylation and as consequence correcting gene expression patterns. Curiously, KAT6A acetylase deficiency was also associated with the down-regulation of NAD^+-dependent deacetylase proteins such as SIRT1 and SIRT3 (as well as NAMT which regulates NAD^+ production, and therefore SIRTs activity) suggesting that KAT6A mutations secondarily leads to a reduction of deacetylase reactions.

 doi:10.20944/preprints202211.0273.v1

In our work, KAT6A mutations also produced a downregulation in the expression levels of PANK2 enzyme and CoA-dependent downstream proteins such as mtACP. Given the essential role of mtACP in lipoic acid biosynthesis [57], mtACP deficiency in mutant cells also led to a decreased lipoylation of key mitochondrial proteins such as PDH and αKGDH and causes mitochondrial dysfunction [58]. In agreement with these data, cell bioenergetics was altered in mutant KAT6A cells. Moreover, mitochondrial dysfunction can lead to several deleterious consequences [59], contributing to the development and progression of cell damage in KAT6A syndrome.

It is interesting to note that although PANK2, mtACP, lipoylated PDH and αKGDH are markedly reduced (Figure 1B), iron is not accumulated in mutant fibroblasts as it has been reported in other disorders [40]. Further studies are needed to clarify the absence of iron accumulation in KAT6A mutant cells.

In KAT6A cellular models, we observed the miss-regulation of thousands of genes (Figure 7), among which many pathway-specific genes are included. As a consequence, the expression levels of genes encoding essential proteins such as KAT6A, SIRT1, SIRT3, NAMPT1, Mt-ND6, NDUFA9, PANK2, mtACP, lipoylated PDH, lipoylated KGDH, SOD1, SOD2 and GPX4 are down-regulated (Figure S14). These proteins are involved in acetylation-deacetylation pathways, CoA metabolism, mitochondria function and antioxidant enzymes. These observations are consistent with several reports, showing that KAT6A is required for the expression of several genes during development [8,11,12,56].

Interestingly, our results also showed that the supplementation with pantothenate and L-carnitine had a positive effect on KAT6A mutant cells associated with the correction of altered protein expression levels, histone acetylation and cell bioenergetics. The beneficial effect of pantothenate and L-carnitine was also confirmed by RNAseq analysis. Thus, the supplementation with both compounds restored the altered pathological expression of genes related to acetylation/methylation and neuronal regulation. In addition, the expression levels of genes encoding down-regulated proteins were restored.

Pantothenate and L-carnitine as epigenetic modulators

Vitamin B5 or pantothenate is the precursor of the CoA biosynthetic pathway [60]. The molecule is largely widespread in biology [61] and in humans, pantothenate deficiency may occur only as a consequence of severe malnutrition. In the cells, CoA synthesis starts with the phosphorylation of pantothenate to 4-phosphopantothenate by PANK. This first reaction represents the major rate-limiting and control step in the entire process of CoA biosynthesis [62]. Pantothenate as a part of CoA forms acetyl-CoA, which is the source of acetyl group in histone acetylation by KAT6A enzyme. Therefore, pantothenate supplementation by increasing acetyl-CoA may facilitate the function of the mutant KAT6A enzyme and therefore correct the defective histone acetylation in mutant cells. This strategy is based on the idea that a functionally weak/mutant enzyme may work better with higher concentrations of its substrate.

L-carnitine is a ubiquitously occurring trimethylated amino acid that plays an important role in the transport of long chain fatty acids across the inner mitochondrial membrane and is of critical importance for maintaining normal mitochondrial function [63,64]. As epigenetic modulator, L-carnitine increases histone acetylation and induces accumulation of acetylated histones both in normal thymocytes and cancer cells [65]; L-carnitine directly inhibits HDAC I/II (Histone deacetylases I/II) activities and induces lysine-acetylation and histone acetylation accumulation in vitro [65]. Furthermore, it has been reported that inhibitors of these HDAC boost mRNA and protein expression of PGC-1α, presumably by promoting transcription of the *PGC-1a* gene [66]; It is therefore proposed that L-carnitine supplementation may provide a moderate tonic inhibition of type 1 HDACs that supports *PGC1α* transcription and promotes mitochondrial biogenesis.

 doi:10.20944/preprints202211.0273.v1

5. Conclusions

In summary, the present work supports the hypothesis that fibroblasts from mutant KAT6A patients are a promising model for the study of the disease pathophysiology and the evaluation of potential treatments.

We showed that the decreased expression level of KAT6A protein directly affects histone acetylation affecting critical intracellular processes such as CoA metabolism, iron metabolism, enzymatic antioxidant system and mitochondrial function. Expression levels of key proteins can be excellent biomarkers to address disease severity and effectiveness of potential therapies. Interestingly, pantothenate and L-carnitine supplementation increased histone acetylation and significantly rescued protein expression levels and all pathological alterations including transcriptional patterns and mitochondrial bioenergetics.

Abbreviations:

AASDHPPT: Aminoadipate semialdehyde dehydrogenase phosphopantetheinyl transferase; AML: Acute myeloid leukemia; ASD: Autism Spectrum disorder; ATCC: American Type Culture Collection; ATP: Adenosine triphosphate; ATP5F1A: ATP Synthase F1 Subunit Alpha; BP: Biological process ontology;BRPF1/2/3: Bromodomain and PHD finger 1/2/3; C1: Control 1; C2: Control 2; CoA: Coenzyme A; COX15: Cytochrome C oxidase subunit 15; COX4: Cytochrome C oxidase subunit 4; DAPI: 4′,6-diamidino-2-phenylindole; DMEM: Dulbecco's modified eagle medium; DMT1: Divalent metal transporter 1; EDTA: Ethylene diamine tetra acetate; FBS: Fetal Bovine Serum; FCCP: Carbonyl cyanide 4-(trifluoromethoxy) phenylhydrazone; FXN: Frataxin; GPX4: Glutathione peroxidase 4; H3K14: Lysine 14 in histone H3; H3K9: Lysine 9 in histone H3; HDAC: Histone deacetylase; hEAF6: Human Esa1-associated factor 6; ID: Intellectual disability; ING5: Inhibitor of Growth Family member 5; IQ: Intelligence quotient; ISCU: Iron-sulfur cluster assembly enzyme; KAT5: Lysine acetyltransferase 5; KAT6A/MOZ: Lysine acetyltransferase 6 A; KAT6B: Lysine acetyltransferase 6 B; KAT7: Lysine acetyltransferase 7; KEGG: Kyoto encyclopedia of genes and genomes; KGDH: α-ketoglutarate dehydrogenase;; LoF: Loss of function; MOI: Multiplicity of infection; mtACP: Mitochondrial acyl carrier protein; MT-ND6: Ubiquinone oxidoreductase core subunit 6; NAD^+: Nicotinamide adenine dinucleotide oxidated; NADH: Nicotinamide adenine dinucleotide reduced; NAMPT1: Nicotinamide phosphoribosyltransferase 1; NCOA4/ARA70: Nuclear receptor coactivator 4; NDUFA9: Ubiquinone oxidoreductase subunit A9; NFS1: Nitrogen fixation 1; NGS: Next-generation sequencing; OCR: Oxygen consumption rate; P1: Patient 1; P2: Patient 2; P3: Patient 3; PANK2: Pantothenate kinase 2; PBS: Phosphate Buffered Saline; PCA: Principal Component Analysis; PDH: Pyruvate dehydrogenase; PGC-1α: Peroxisome proliferator-activated receptor gamma coactivator 1-alpha; REST: RE1-silencing transcription factor; RNA-seq: RNA sequencing; ROS: Reactive oxygen species; SIRT1: Sirtuin 1; SIRT3: Sirtuin 3; SM: Serine and methionine rich domain; SOD1: Superoxide dismutase 1; SOD2: Superoxide dismutase 2; TfR: Transferrin receptor; VDAC1: Voltage-dependent anion-selective channel protein 1.

Supplementary Materials: Figure S1: Western blotting quantification of figure 1. Band densitometry of western blot shown in figure 1; Figure S2: Western blotting quantification of figure 1. Pathways in figure panels; Figure S3: Iron accumulation in control (C1 and C2) and mutant KAT6A fibroblasts (P1, P2 and P3) assessed by Prussian Blue staining (A). Quantification of Prussian Blue staining of controls and patient fibroblasts (B); Figure S4: (A) Cell quantification control (C1) and mutant KAT6A fibroblasts in galactose medium with oligomycin at 0.5 nM (O). (B) Cell proliferation rate obtained from Nº Cells at T72h (T1)/ Nº cells at T0h (T0); Figure S5: (A) Cell quantification of control (C1) and mutant KAT6A fibroblasts in galactose medium with oligomycin at 0,5 nM (O). (A) Cell proliferation rate was obtained by the equation: Nº Cells at T72h (T1)/ Nº cells at T0h (T0). (B) Results ≥ 1 indicate cell survival and proliferation; Figure S6: (A) Cell quantification control (C1) and mutant KAT6A fibroblasts in galactose medium with oligomycin at 0.5 nM (O). (B) Cell proliferation rate was obtained by the equation: Nº Cells at T72h (T1)/ Nº cells at T0h (T0); Figure S7: Western blotting quantification of figure 3; Figure S8: Western blotting quantification of figure 3; Figure S9: Quantification of H3K9/K14 Acetylation and MitoTracker staining of figure 4 using softWoRx and ImageJ software; Figure S10: Effect of 0.4 μM pantothenate and 0.4 μM L-carnitine on histone acetylation levels in control (C) and KAT6A fibroblasts (Patient 2 – P2); Figure S11: Effect of 0.7 μM pantothenate and 0.7 μM L-carnitine on histone acetylation levels in control (C) and KAT6A fibroblasts (Patient 3 – P3); Figure S12: Effect of pantothenate and L-carnitine supplementation on

mitostress bioenergetic assay in control (control – C1) and mutant KAT6A fibroblasts (Patient 2- P2); Figure S13: Effect of pantothenate and L-carnitine supplementation on mitostress bioenergetic assay in control (control – C1) and mutant KAT6A fibroblasts (Patient 3- P3).; Figure S14: Transcript expression levels of key altered genes in control and mutant KAT6A fibroblasts with and without pantothenate and L-carnitine treatment; Figure S15: Quality control in control and mutant KAT6A fibroblasts treated and non treated with a Phred-Score (Q) greater than 30.

Author Contributions: Conceptualization, M.M-C. and J.A.S-A.; methodology, M.M-C., J.M.S-R-. and M.A-C..; software, A.S-C. and S.P-C..; validation, P.C-H., D.R-L., and R.P-P. ; investigation, I.V-G..;; writing—original draft preparation, M.M-C. and J.A.S-A.; writing—review and editing, M.M-C. and J.A.S-A.; funding acquisition, J.A.S-A All authors have read and agreed to the published version of the manuscript.

Funding: This research was funded by FIS PI16/00786 (2016) and FIS PI19/00377 (2019) grants, the Ministerio de Sanidad, Spain and the Fondo Europeo de Desarrollo Regional (FEDER Unión Europea), Spanish Ministry of Education, Culture and Sport. This activity has been co-financed by the European Regional Development Fund (ERDF) and by the Regional Ministry of Economic Transformation, Industry, Knowledge and Universities of the Junta de Andalucía, within the framework of the ERDF Andalusia operational program 2014-2020 Thematic objective "01 - Reinforcement of research, technological development and innovation" through the reference research project CTS-5725 and PY18-850.

Institutional Review Board Statement: The study was approved by The Ethical Committee of Hospital Universitario Virgen del Rocío and Virgen Macarena of Seville, protocol code MITOCURE, following the Spanish laws, the principles of the Declaration of Helsinki, and the Guideline for Good Clinical Practices.

Informed Consent Statement: Informed consent was obtained from all subjects involved in the study

Data Availability Statement: The data presented in this study are available in the article and supplementary material.

Acknowledgments: We acknowledge the support of "Ayudas para la Formación de Profesorado Universitario" (FPU/MINECO), Superauténticos Association, Spanish KAT6A Association, KAT6A Foundation and Fundación MEHUER/ Colegio Oficial de Farmacéuticos de Sevilla.

Conflicts of Interest: The authors declare no conflict of interest.

References

1. Kennedy, J.; Goudie, D.; Blair, E.; Chandler, K.; Joss, S.; McKay, V.; Green, A.; Armstrong, R.; Lees, M.; Kamien, B., et al. KAT6A Syndrome: genotype-phenotype correlation in 76 patients with pathogenic KAT6A variants. *Genet Med* **2019**, *21*, 850-860, doi:10.1038/s41436-018-0259-2.
2. Lee, H.; Deignan, J.L.; Dorrani, N.; Strom, S.P.; Kantarci, S.; Quintero-Rivera, F.; Das, K.; Toy, T.; Harry, B.; Yourshaw, M., et al. Clinical exome sequencing for genetic identification of rare Mendelian disorders. *JAMA* **2014**, *312*, 1880-1887, doi:10.1001/jama.2014.14604.
3. Arboleda, V.A.; Lee, H.; Dorrani, N.; Zadeh, N.; Willis, M.; Macmurdo, C.F.; Manning, M.A.; Kwan, A.; Hudgins, L.; Barthelemy, F., et al. De novo nonsense mutations in KAT6A, a lysine acetyl-transferase gene, cause a syndrome including microcephaly and global developmental delay. *Am J Hum Genet* **2015**, *96*, 498-506, doi:10.1016/j.ajhg.2015.01.017.
4. Tham, E.; Lindstrand, A.; Santani, A.; Malmgren, H.; Nesbitt, A.; Dubbs, H.A.; Zackai, E.H.; Parker, M.J.; Millan, F.; Rosenbaum, K., et al. Dominant mutations in KAT6A cause intellectual disability with recognizable syndromic features. *Am J Hum Genet* **2015**, *96*, 507-513, doi:10.1016/j.ajhg.2015.01.016.
5. Millan, F.; Cho, M.T.; Retterer, K.; Monaghan, K.G.; Bai, R.; Vitazka, P.; Everman, D.B.; Smith, B.; Angle, B.; Roberts, V., et al. Whole exome sequencing reveals de novo pathogenic variants in KAT6A as a cause of a neurodevelopmental disorder. *Am J Med Genet A* **2016**, *170*, 1791-1798, doi:10.1002/ajmg.a.37670.
6. Fahrner, J.A.; Bjornsson, H.T. Mendelian disorders of the epigenetic machinery: tipping the balance of chromatin states. *Annu Rev Genomics Hum Genet* **2014**, *15*, 269-293, doi:10.1146/annurev-genom-090613-094245.
7. Avvakumov, N.; Cote, J. The MYST family of histone acetyltransferases and their intimate links to cancer. *Oncogene* **2007**, *26*, 5395-5407, doi:10.1038/sj.onc.1210608.
8. Voss, A.K.; Vanyai, H.K.; Collin, C.; Dixon, M.P.; McLennan, T.J.; Sheikh, B.N.; Scambler, P.; Thomas, T. MOZ regulates the Tbx1 locus, and Moz mutation partially phenocopies DiGeorge syndrome. *Dev Cell* **2012**, *23*, 652-663, doi:10.1016/j.devcel.2012.07.010.
9. Yang, X.J. MOZ and MORF acetyltransferases: Molecular interaction, animal development and human disease. *Biochim Biophys Acta* **2015**, *1853*, 1818-1826, doi:10.1016/j.bbamcr.2015.04.014.

10. Rozman, M.; Camos, M.; Colomer, D.; Villamor, N.; Esteve, J.; Costa, D.; Carrio, A.; Aymerich, M.; Aguilar, J.L.; Domingo, A., et al. Type I MOZ/CBP (MYST3/CREBBP) is the most common chimeric transcript in acute myeloid leukemia with t(8;16)(p11;p13) translocation. *Genes Chromosomes Cancer* **2004**, *40*, 140-145, doi:10.1002/gcc.20022.
11. Rokudai, S.; Laptenko, O.; Arnal, S.M.; Taya, Y.; Kitabayashi, I.; Prives, C. MOZ increases p53 acetylation and premature senescence through its complex formation with PML. *Proc Natl Acad Sci U S A* **2013**, *110*, 3895-3900, doi:10.1073/pnas.1300490110.
12. Pelletier, N.; Champagne, N.; Stifani, S.; Yang, X.J. MOZ and MORF histone acetyltransferases interact with the Runt-domain transcription factor Runx2. *Oncogene* **2002**, *21*, 2729-2740, doi:10.1038/sj.onc.1205367.
13. Trinh, J.; Huning, I.; Yuksel, Z.; Baalmann, N.; Imhoff, S.; Klein, C.; Rolfs, A.; Gillessen-Kaesbach, G.; Lohmann, K. A KAT6A variant in a family with autosomal dominantly inherited microcephaly and developmental delay. *J Hum Genet* **2018**, *63*, 997-1001, doi:10.1038/s10038-018-0469-0.
14. Perez-Campo, F.M.; Borrow, J.; Kouskoff, V.; Lacaud, G. The histone acetyl transferase activity of monocytic leukemia zinc finger is critical for the proliferation of hematopoietic precursors. *Blood* **2009**, *113*, 4866-4874, doi:10.1182/blood-2008-04-152017.
15. Sapountzi, V.; Cote, J. MYST-family histone acetyltransferases: beyond chromatin. *Cell Mol Life Sci* **2011**, *68*, 1147-1156, doi:10.1007/s00018-010-0599-9.
16. Thomas, T.; Corcoran, L.M.; Gugasyan, R.; Dixon, M.P.; Brodnicki, T.; Nutt, S.L.; Metcalf, D.; Voss, A.K. Monocytic leukemia zinc finger protein is essential for the development of long-term reconstituting hematopoietic stem cells. *Genes Dev* **2006**, *20*, 1175-1186, doi:10.1101/gad.1382606.
17. Good-Jacobson, K.L.; Chen, Y.; Voss, A.K.; Smyth, G.K.; Thomas, T.; Tarlinton, D. Regulation of germinal center responses and B-cell memory by the chromatin modifier MOZ. *Proc Natl Acad Sci U S A* **2014**, *111*, 9585-9590, doi:10.1073/pnas.1402485111.
18. Newman, D.M.; Sakaguchi, S.; Lun, A.; Preston, S.; Pellegrini, M.; Khamina, K.; Bergthaler, A.; Nutt, S.L.; Smyth, G.K.; Voss, A.K., et al. Acetylation of the Cd8 Locus by KAT6A Determines Memory T Cell Diversity. *Cell Rep* **2016**, *16*, 3311-3321, doi:10.1016/j.celrep.2016.08.056.
19. Villalon-Garcia, I.; Alvarez-Cordoba, M.; Suarez-Rivero, J.M.; Povea-Cabello, S.; Talaveron-Rey, M.; Suarez-Carrillo, A.; Munuera-Cabeza, M.; Sanchez-Alcazar, J.A. Precision Medicine in Rare Diseases. *Diseases* **2020**, *8*, doi:10.3390/diseases8040042.
20. Connolly, G.P. Fibroblast models of neurological disorders: fluorescence measurement studies. *Trends Pharmacol Sci* **1998**, *19*, 171-177, doi:10.1016/s0165-6147(98)01202-4.
21. Gershlick, D.C.; Ishida, M.; Jones, J.R.; Bellomo, A.; Bonifacino, J.S.; Everman, D.B. A neurodevelopmental disorder caused by mutations in the VPS51 subunit of the GARP and EARP complexes. *Hum Mol Genet* **2019**, *28*, 1548-1560, doi:10.1093/hmg/ddy423.
22. Milev, M.P.; Graziano, C.; Karall, D.; Kuper, W.F.E.; Al-Deri, N.; Cordelli, D.M.; Haack, T.B.; Danhauser, K.; Iuso, A.; Palombo, F., et al. Bi-allelic mutations in TRAPPC2L result in a neurodevelopmental disorder and have an impact on RAB11 in fibroblasts. *J Med Genet* **2018**, *55*, 753-764, doi:10.1136/jmedgenet-2018-105441.
23. Olesen, M.A.; Villavicencio-Tejo, F.; Quintanilla, R.A. The use of fibroblasts as a valuable strategy for studying mitochondrial impairment in neurological disorders. *Transl Neurodegener* **2022**, *11*, 36, doi:10.1186/s40035-022-00308-y.
24. Sbardella, D.; Tundo, G.R.; Campagnolo, L.; Valacchi, G.; Orlandi, A.; Curatolo, P.; Borsellino, G.; D'Esposito, M.; Ciaccio, C.; Cesare, S.D., et al. Retention of Mitochondria in Mature Human Red Blood Cells as the Result of Autophagy Impairment in Rett Syndrome. *Sci Rep* **2017**, *7*, 12297, doi:10.1038/s41598-017-12069-0.
25. Adzhubei, I.; Jordan, D.M.; Sunyaev, S.R. Predicting functional effect of human missense mutations using PolyPhen-2. *Curr Protoc Hum Genet* **2013**, *Chapter 7*, Unit7 20, doi:10.1002/0471142905.hg0720s76.
26. Alvarez-Cordoba, M.; Fernandez Khoury, A.; Villanueva-Paz, M.; Gomez-Navarro, C.; Villalon-Garcia, I.; Suarez-Rivero, J.M.; Povea-Cabello, S.; de la Mata, M.; Cotan, D.; Talaveron-Rey, M., et al. Pantothenate Rescues Iron Accumulation in Pantothenate Kinase-Associated Neurodegeneration Depending on the Type of Mutation. *Molecular neurobiology* **2019**, *56*, 3638-3656, doi:10.1007/s12035-018-1333-0.
27. Kamalian, L.; Douglas, O.; Jolly, C.E.; Snoeys, J.; Simic, D.; Monshouwer, M.; Williams, D.P.; Park, B.K.; Chadwick, A.E. Acute Metabolic Switch Assay Using Glucose/Galactose Medium in HepaRG Cells to Detect Mitochondrial Toxicity. *Curr Protoc Toxicol* **2019**, *80*, e76, doi:10.1002/cptx.76.
28. Coelho, A.I.; Berry, G.T.; Rubio-Gozalbo, M.E. Galactose metabolism and health. *Curr Opin Clin Nutr Metab Care* **2015**, *18*, 422-427, doi:10.1097/MCO.0000000000000189.
29. Rodriguez-Hernandez, A.; Cordero, M.D.; Salviati, L.; Artuch, R.; Pineda, M.; Briones, P.; Gomez Izquierdo, L.; Cotan, D.; Navas, P.; Sanchez-Alcazar, J.A. Coenzyme Q deficiency triggers mitochondria degradation by mitophagy. *Autophagy* **2009**, *5*, 19-32, doi:10.4161/auto.5.1.7174.
30. Bolger, A.M.; Lohse, M.; Usadel, B. Trimmomatic: a flexible trimmer for Illumina sequence data. *Bioinformatics* **2014**, *30*, 2114-2120, doi:10.1093/bioinformatics/btu170.
31. Langmead, B.; Salzberg, S.L. Fast gapped-read alignment with Bowtie 2. *Nat Methods* **2012**, *9*, 357-359, doi:10.1038/nmeth.1923.
32. Garcia-Alcalde, F.; Okonechnikov, K.; Carbonell, J.; Cruz, L.M.; Gotz, S.; Tarazona, S.; Dopazo, J.; Meyer, T.F.; Conesa, A. Qualimap: evaluating next-generation sequencing alignment data. *Bioinformatics* **2012**, *28*, 2678-2679, doi:10.1093/bioinformatics/bts503.
33. Liao, Y.; Smyth, G.K.; Shi, W. featureCounts: an efficient general purpose program for assigning sequence reads to genomic features. *Bioinformatics* **2014**, *30*, 923-930, doi:10.1093/bioinformatics/btt656.
34. Love, M.I.; Huber, W.; Anders, S. Moderated estimation of fold change and dispersion for RNA-seq data with DESeq2. *Genome Biol* **2014**, *15*, 550, doi:10.1186/s13059-014-0550-8.

35. Merico, D.; Isserlin, R.; Stueker, O.; Emili, A.; Bader, G.D. Enrichment map: a network-based method for gene-set enrichment visualization and interpretation. *PLoS One* **2010**, *5*, e13984, doi:10.1371/journal.pone.0013984.
36. Suarez-Rivero, J.M.; Pastor-Maldonado, C.J.; Romero-Gonzalez, A.; Gomez-Fernandez, D.; Povea-Cabello, S.; Alvarez-Cordoba, M.; Villalon-Garcia, I.; Talaveron-Rey, M.; Suarez-Carrillo, A.; Munuera-Cabeza, M., et al. Pterostilbene in Combination With Mitochondrial Cofactors Improve Mitochondrial Function in Cellular Models of Mitochondrial Diseases. *Front Pharmacol* **2022**, *13*, 862085, doi:10.3389/fphar.2022.862085.
37. Suarez-Rivero, J.M.; Pastor-Maldonado, C.J.; Povea-Cabello, S.; Alvarez-Cordoba, M.; Villalon-Garcia, I.; Talaveron-Rey, M.; Suarez-Carrillo, A.; Munuera-Cabeza, M.; Reche-Lopez, D.; Cilleros-Holgado, P., et al. UPR(mt) activation improves pathological alterations in cellular models of mitochondrial diseases. *Orphanet J Rare Dis* **2022**, *17*, 204, doi:10.1186/s13023-022-02331-8.
38. Villanueva-Paz, M.; Povea-Cabello, S.; Villalon-Garcia, I.; Alvarez-Cordoba, M.; Suarez-Rivero, J.M.; Talaveron-Rey, M.; Jackson, S.; Falcon-Moya, R.; Rodriguez-Moreno, A.; Sanchez-Alcazar, J.A. Parkin-mediated mitophagy and autophagy flux disruption in cellular models of MERRF syndrome. *Biochim Biophys Acta Mol Basis Dis* **2020**, *1866*, 165726, doi:10.1016/j.bbadis.2020.165726.
39. Le Boedec, K. Sensitivity and specificity of normality tests and consequences on reference interval accuracy at small sample size: a computer-simulation study. *Vet Clin Pathol* **2016**, *45*, 648-656, doi:10.1111/vcp.12390.
40. Alvarez-Cordoba, M.; Talaveron-Rey, M.; Villalon-Garcia, I.; Povea-Cabello, S.; Suarez-Rivero, J.M.; Suarez-Carrillo, A.; Munuera-Cabeza, M.; Salas, J.J.; Sanchez-Alcazar, J.A. Down regulation of the expression of mitochondrial phosphopantetheinyl-proteins in pantothenate kinase-associated neurodegeneration: pathophysiological consequences and therapeutic perspectives. *Orphanet J Rare Dis* **2021**, *16*, 201, doi:10.1186/s13023-021-01823-3.
41. Joshi, A.K.; Zhang, L.; Rangan, V.S.; Smith, S. Cloning, expression, and characterization of a human 4'-phosphopantetheinyl transferase with broad substrate specificity. *J Biol Chem* **2003**, *278*, 33142-33149, doi:10.1074/jbc.M305459200.
42. Shoshan-Barmatz, V.; Ben-Hail, D. VDAC, a multi-functional mitochondrial protein as a pharmacological target. *Mitochondrion* **2012**, *12*, 24-34, doi:10.1016/j.mito.2011.04.001.
43. Yang, X.J. The diverse superfamily of lysine acetyltransferases and their roles in leukemia and other diseases. *Nucleic Acids Res* **2004**, *32*, 959-976, doi:10.1093/nar/gkh252.
44. Berger, S.L. Histone modifications in transcriptional regulation. *Curr Opin Genet Dev* **2002**, *12*, 142-148, doi:10.1016/s0959-437x(02)00279-4.
45. Glass, C.K.; Rosenfeld, M.G. The coregulator exchange in transcriptional functions of nuclear receptors. *Genes Dev* **2000**, *14*, 121-141.
46. Taatjes, D.J.; Marr, M.T.; Tjian, R. Regulatory diversity among metazoan co-activator complexes. *Nat Rev Mol Cell Biol* **2004**, *5*, 403-410, doi:10.1038/nrm1369.
47. Howe, L.; Auston, D.; Grant, P.; John, S.; Cook, R.G.; Workman, J.L.; Pillus, L. Histone H3 specific acetyltransferases are essential for cell cycle progression. *Genes Dev* **2001**, *15*, 3144-3154, doi:10.1101/gad.931401.
48. Katsumoto, T.; Aikawa, Y.; Iwama, A.; Ueda, S.; Ichikawa, H.; Ochiya, T.; Kitabayashi, I. MOZ is essential for maintenance of hematopoietic stem cells. *Genes Dev* **2006**, *20*, 1321-1330, doi:10.1101/gad.1393106.
49. Sheikh, B.N.; Lee, S.C.; El-Saafin, F.; Vanyai, H.K.; Hu, Y.; Pang, S.H.; Grabow, S.; Strasser, A.; Nutt, S.L.; Alexander, W.S., et al. MOZ regulates B-cell progenitors and, consequently, Moz haploinsufficiency dramatically retards MYC-induced lymphoma development. *Blood* **2015**, *125*, 1910-1921, doi:10.1182/blood-2014-08-594655.
50. Huang, F.; Abmayr, S.M.; Workman, J.L. Regulation of KAT6 Acetyltransferases and Their Roles in Cell Cycle Progression, Stem Cell Maintenance, and Human Disease. *Mol Cell Biol* **2016**, *36*, 1900-1907, doi:10.1128/MCB.00055-16.
51. Sheikh, B.N.; Phipson, B.; El-Saafin, F.; Vanyai, H.K.; Downer, N.L.; Bird, M.J.; Kueh, A.J.; May, R.E.; Smyth, G.K.; Voss, A.K., et al. MOZ (MYST3, KAT6A) inhibits senescence via the INK4A-ARF pathway. *Oncogene* **2015**, *34*, 5807-5820, doi:10.1038/onc.2015.33.
52. Strahl, B.D.; Allis, C.D. The language of covalent histone modifications. *Nature* **2000**, *403*, 41-45, doi:10.1038/47412.
53. Eberharter, A.; Becker, P.B. Histone acetylation: a switch between repressive and permissive chromatin. Second in review series on chromatin dynamics. *EMBO Rep* **2002**, *3*, 224-229, doi:10.1093/embo-reports/kvf053.
54. Voss, A.K.; Collin, C.; Dixon, M.P.; Thomas, T. Moz and retinoic acid coordinately regulate H3K9 acetylation, Hox gene expression, and segment identity. *Dev Cell* **2009**, *17*, 674-686, doi:10.1016/j.devcel.2009.10.006.
55. Kitabayashi, I.; Aikawa, Y.; Nguyen, L.A.; Yokoyama, A.; Ohki, M. Activation of AML1-mediated transcription by MOZ and inhibition by the MOZ-CBP fusion protein. *EMBO J* **2001**, *20*, 7184-7196, doi:10.1093/emboj/20.24.7184.
56. Bristow, C.A.; Shore, P. Transcriptional regulation of the human MIP-1alpha promoter by RUNX1 and MOZ. *Nucleic Acids Res* **2003**, *31*, 2735-2744, doi:10.1093/nar/gkg401.
57. Hiltunen, J.K.; Schonauer, M.S.; Autio, K.J.; Mittelmeier, T.M.; Kastaniotis, A.J.; Dieckmann, C.L. Mitochondrial fatty acid synthesis type II: more than just fatty acids. *J Biol Chem* **2009**, *284*, 9011-9015, doi:10.1074/jbc.R800068200.
58. Cronan, J.E. Assembly of Lipoic Acid on Its Cognate Enzymes: an Extraordinary and Essential Biosynthetic Pathway. *Microbiol Mol Biol Rev* **2016**, *80*, 429-450, doi:10.1128/MMBR.00073-15.
59. Millichap, L.E.; Damiani, E.; Tiano, L.; Hargreaves, I.P. Targetable Pathways for Alleviating Mitochondrial Dysfunction in Neurodegeneration of Metabolic and Non-Metabolic Diseases. *Int J Mol Sci* **2021**, *22*, doi:10.3390/ijms222111444.
60. Mignani, L.; Gnutti, B.; Zizioli, D.; Finazzi, D. Coenzyme a Biochemistry: From Neurodevelopment to Neurodegeneration. *Brain Sci* **2021**, *11*, doi:10.3390/brainsci11081031.

61. Tahiliani, A.G.; Beinlich, C.J. Pantothenic acid in health and disease. *Vitamins and hormones* **1991**, *46*, 165-228, doi:10.1016/s0083-6729(08)60684-6.
62. Rock, C.O.; Calder, R.B.; Karim, M.A.; Jackowski, S. Pantothenate kinase regulation of the intracellular concentration of coenzyme A. *J Biol Chem* **2000**, *275*, 1377-1383, doi:10.1074/jbc.275.2.1377.
63. Bremer, J. Carnitine--metabolism and functions. *Physiological reviews* **1983**, *63*, 1420-1480, doi:10.1152/physrev.1983.63.4.1420.
64. Jacob, C.; Belleville, F. [L-carnitine: metabolism, functions and value in pathology]. *Pathologie-biologie* **1992**, *40*, 910-919.
65. Huang, H.; Liu, N.; Guo, H.; Liao, S.; Li, X.; Yang, C.; Liu, S.; Song, W.; Liu, C.; Guan, L., et al. L-carnitine is an endogenous HDAC inhibitor selectively inhibiting cancer cell growth in vivo and in vitro. *PLoS One* **2012**, *7*, e49062, doi:10.1371/journal.pone.0049062.
66. McCarty, M.; DiNicolantonio, J.J.; #039; Keefe, J.H. The Ability of Carnitine to Act as a Type 1Histone Deacetylase Inhibitor May Explain the Favorable Impact of Carnitine Supplementation on Mitochondrial Biogenesis in the Elderly. *Medical Research Archives* **2020**, *8*, doi:10.18103/mra.v8i2.2055.